## SUPPLEMENTAL INFORMATION

### Effective free energy and induced DM term

Let us consider the following low energy Hamiltonian for the Dirac fermions on the surface of the TI,

$$H_{\rm Dirac}=[\mathbf{d}\left(-i\hbar\boldsymbol{\nabla}\right)-J_0\mathbf{n}(\mathbf{r})]\cdot\boldsymbol{\sigma}. \tag{S1}$$

Quite generally, the non-interacting Green function for a spin-momentum locked system can be written,

$$\mathcal{G}_{\alpha\beta}(X)=G(X)\delta_{\alpha\beta}+\mathbf{F}(X)\cdot\boldsymbol{\sigma}_{\alpha\beta}, \tag{S2}$$

where $X=(\tau,\mathbf{r})$, with $\tau\in[0,\beta]$ being the imaginary time. Thus, expanding the free energy expression up to $J_0^2$, we obtain $F_{\rm Dirac}=F_{\rm Dirac}(0)+\delta F_{\rm Dirac}$, where,

$$\delta F_{\rm Dirac}=\frac{1}{2}\int_X\int_{X'}\mathcal{G}_{\alpha\beta}(X-X')\mathcal{G}_{\gamma\delta}(X'-X)[J_0\mathbf{n}(X)\cdot\boldsymbol{\sigma}_{\beta\gamma}][J_0\mathbf{n}(X')\cdot\boldsymbol{\sigma}_{\delta\alpha}], \tag{S3}$$

where we use the shorthand notation $\int_X\equiv\int_0^\beta d\tau\int d^2r$. Lengthy but straightforward calculations yield,

$$\delta F_{\rm Dirac}^{\rm mag}=\frac{J_0^2}{2}\int_X\int_{X'}\{2[G(X-X')G(X'-X)-\mathbf{F}(X-X')\cdot\mathbf{F}(X'-X)]\mathbf{n}(X)\cdot\mathbf{n}(X')$$
$$+4\mathbf{F}(X-X')\cdot\mathbf{n}(X)\mathbf{F}(X'-X)\cdot\mathbf{n}(X')-24iG(X-X')\mathbf{F}(X'-X)\cdot[\mathbf{n}(X)\times\mathbf{n}(X')]\}, \tag{S4}$$

where in writing the above equation we have made use of the property $\mathbf{F}(\tau,-\mathbf{r})=-\mathbf{F}(\tau,\mathbf{r})$.

Observe that Eq. (S4) features also the general Dzyloshinsky-Moriya (DM) term, which arises in the third line of that equation. It can be re-cast in a more familiar form by specializing to the simple case,

$$G(\omega_n,\mathbf{k})=\frac{i\omega_n+\mu}{(i\omega_n+\mu)^2-\mathbf{d}^2(\mathbf{k})}, \tag{S5}$$

$$\mathbf{F}(\omega_n,\mathbf{k})=-\frac{\mathbf{d}(\mathbf{k})}{(i\omega_n+\mu)^2-\mathbf{d}^2(\mathbf{k})}, \tag{S6}$$

where $\omega_n=(2n+1)\pi/\beta$ and $\mathbf{d}(\mathbf{k})$ is either $\mathbf{d}_1$ or $\mathbf{d}_2$ from Eq. (2) in momentum space. Assuming a time-independent magnetization, Eq. (S4) becomes,

$$\delta F_{\rm Dirac}^{\rm mag}=\frac{J_0^2}{2}\int\frac{d^2k}{(2\pi)^2}[S_{ab}(\mathbf{k})+A_c(\mathbf{k})\epsilon_{abc}]n_a(\mathbf{k})n_b(-\mathbf{k}), \tag{S7}$$

featuring symmetric and antisymmetric contributions $S_{ab}$ and $A_c$, which are given by,

$$S_{ab}(\mathbf{k})=\frac{2}{\beta}\sum_{n=-\infty}^{\infty}\int\frac{d^2q}{(2\pi)^2}\frac{[(i\omega_n+\mu)^2-\mathbf{d}(\mathbf{q})\cdot\mathbf{d}(\mathbf{q}+\mathbf{k})]\delta_{ab}+2d_a(\mathbf{q})d_b(\mathbf{q}+\mathbf{k})}{[(i\omega_n+\mu)^2-(\hbar v_F)^2q^2][(i\omega_n+\mu)^2-(\hbar v_F)^2(\mathbf{q}+\mathbf{k})^2]}, \tag{S8}$$

$$A_c(\mathbf{k})=\frac{24i}{\beta}\sum_{n=-\infty}^{\infty}\int\frac{d^2q}{(2\pi)^2}\frac{(i\omega_n+\mu)d_c(\mathbf{q})}{[(i\omega_n+\mu)^2-(\hbar v_F)^2q^2][(i\omega_n+\mu)^2-(\hbar v_F)^2(\mathbf{q}+\mathbf{k})^2]}, \tag{S9}$$

respectively.

The symmetric contribution induces a magnetization stiffness at the interface. Part of the integral yielding $S_{ab}$ does not converge and needs to be regularized by means of a cutoff $\Lambda$. The result in the long wavelength limit is,

$$S_{ab}(\mathbf{k})=-\frac{\Lambda}{4\pi\hbar v_F}\delta_{ab}+\mathcal{S}(\beta,\mu)k^2\left(\delta_{ab}+\frac{k_ak_b}{k^2}\right), \tag{S10}$$

where $\mathcal{S}(\beta,\mu)=\beta/[24\pi\cosh^2(\beta\mu/2)]$.

The antisymmetric contribution vanishes for $\mu=0$, since the Matsubara sum involves an odd summand in this case. Thus, in order to generate a DM term the chemical potential must be nonzero. Assuming $\mu\neq 0$, and a long wavelength limit, we obtain,

$$A_c(\mathbf{k})=-id_c(\mathbf{k})\mathcal{A}(\beta\mu), \tag{S11}$$

where $\mathcal{A}(\beta\mu)=3(\pi\hbar v_F)^{-1}\tanh(\beta\mu/2)$. Writing,

$$F_{\rm Dirac}^{\rm mag}=\int d^2r\mathcal{F}_{\rm Dirac}^{\rm mag}(\mathbf{n}(\mathbf{r})), \tag{S12}$$

we obtain for the fluctuation correction of the free energy density,

$$\delta\mathcal{F}^{\rm mag}_{\rm Dirac} = \frac{s}{2}\left\{[\boldsymbol{\nabla}\mathbf{n}(\mathbf{r})]^2 + [\boldsymbol{\nabla}\cdot\mathbf{n}(\mathbf{r})]^2\right\} + i\frac{a}{2}\mathbf{n}(\mathbf{r})\cdot[\mathbf{d}(-i\hbar\boldsymbol{\nabla})\times\mathbf{n}(\mathbf{r})], \tag{S13}$$

where $(\boldsymbol{\nabla}\mathbf{n})^2 = \sum_{i=x,y,z}(\boldsymbol{\nabla}n_i)^2$ defines the usual exchange term, and we have defined $s = J_0^2\mathcal{S}(\beta,\mu)$ and $a = J_0^2\mathcal{A}(\beta,\mu)$. A term proportional to $\Lambda\mathbf{n}^2$ implied by the first term in (S10) has been removed, since it is actually a constant in view of the constraint $\mathbf{n}^2 = 1$. Similarly, we can drop the constant term $F_{\rm Dirac}(0)$ from the free energy, since it does not depend on the field. Thus, we can safely write $\mathcal{F}_{\rm Dirac} = \delta\mathcal{F}_{\rm Dirac}$. The above expression features a DM term induced by Dirac fermion fluctuations. In addition, a contribution $\sim(\boldsymbol{\nabla}\cdot\mathbf{n})^2$ is also generated. This term leads to interesting physical properties when $\mathbf{d}_2$ is replaced for $\mathbf{d}$ in Eq. (S13), modifying in this way the behavior of Néel skyrmions. Note that differently from the case where the Dirac fermion is gapped [1], no intrinsic anisotropy is generated by the Dirac fermions.

### One-dimensional magnetization modulation

Here we consider one-dimensional static solutions $\mathbf{n} = \mathbf{n}(x)$ of the model (8). Let us start with the case $\mathscr{E}_{\rm DMI} = \mathscr{E}^{\rm N}_{\rm DMI}$. In this case the effective energy $E_{\rm eff} = AL\int\mathcal{E}^{\rm N}_{\rm 1D}{\rm d}^2x$ is described by the density

$$\mathcal{E}^{\rm N}_{\rm 1D} = \theta'^2 + \sin^2\theta\phi'^2 + \epsilon\left(\cos\theta\cos\phi\theta' - \sin\theta\sin\phi\phi'\right)^2 + d\left(\cos\phi\theta' - \sin\theta\cos\theta\sin\phi\phi'\right) + 2(1-\cos\theta), \tag{S14}$$

where angles $\theta(x)$ and $\phi(x)$ determine orientation of the unit magnetization vector $\mathbf{n} = \sin\theta(\cos\phi\,\hat{\boldsymbol{x}} + \sin\phi\,\hat{\boldsymbol{y}}) + \cos\theta\hat{\boldsymbol{z}}$, prime denotes the derivation with respect to the dimensionless coordinate $x$ measured in units of $\ell$. The corresponding Euler-Lagrange equations $\delta E_{\rm eff}/\delta\theta = 0$ and $\delta E_{\rm eff}/\delta\phi = 0$ are as follows

$$\theta'' - \sin\theta\cos\theta\phi'^2 - \epsilon\cos\theta\cos\phi\,\Xi - d\sin^2\theta\sin\phi\phi' - \sin\theta = 0, \tag{S15a}$$

$$\left(\sin^2\theta\phi'\right)' + \epsilon\sin\theta\sin\phi\,\Xi + d\sin^2\theta\sin\phi\theta' = 0, \tag{S15b}$$

where

$$\Xi = \cos\theta\left[2\sin\phi\,\theta'\phi' - \cos\phi\,\theta''\right] + \sin\theta\left[\cos\phi\left(\theta'^2+\phi'^2\right) + \sin\phi\,\phi''\right]. \tag{S15c}$$

First of all, Eqs. (S15) have trivial solution $\theta = 0$, which corresponds to the uniform magnetization along the field $\mathbf{n} = \hat{\boldsymbol{z}}$. The uniform state has zero energy $\mathcal{E}^{\rm N}_{\rm 1D} = 0$. The another trivial solution $\theta = \pi$ ($\mathbf{n} = -\hat{\boldsymbol{z}}$) corresponds to the energy maximum and it is unstable.

Let us consider possible nonuniform solutions. Equation (S15b) is satisfied when $\sin\phi = 0$ ($\phi = 0$ for $d\theta' < 0$, and $\phi = \pi$ for $d\theta' > 0$), or in the other words $\mathrm{n}_y = 0$. Thus, the magnetization lies within the plane $\hat{\boldsymbol{x}}0\hat{\boldsymbol{z}}$. The components $\mathrm{n}_x = \sin\theta$ and $\mathrm{n}_z = \cos\theta$ are determined by the equation (S15a), which now looks has a form

$$\theta''\left(1+\epsilon\cos^2\theta\right) = \sin\theta\left(1+\epsilon\cos\theta\theta'^2\right), \tag{S16}$$

and the corresponding energy density reads

$$\mathcal{E} = \theta'^2(1+\epsilon\cos^2\theta) + 4\sin^2\frac{\theta}{2} - d\theta', \tag{S17}$$

where we assumed that $d\theta' > 0$. Rewriting the Eq. (S16) in form $\left[\theta'^2(1+\epsilon\cos^2\theta)\right]' = -2(\cos\theta)'$ one can easily find its first integral

$$\theta'^2(1+\epsilon\cos^2\theta) = 4\sin^2\frac{\theta}{2} + 4C, \tag{S18}$$

where $C$ is the integration constant. Equation (S18) admits separation of the variables and can be solved in quadratures. The constant $C$ determines period $T$ of the magnetization structure: $\mathbf{n}(x+T) = \mathbf{n}(x)$. Let us first consider the particular case $C = 0$, it corresponds to a solution of (S18), which satisfies the boundary conditions $\theta(-\infty) = 0$, $\theta(+\infty) = 2\pi$ (or vice-versa), this is a single $2\pi$-domain wall of Néel type, in this case $T\to\infty$. Taking into account (S18) and (S17) one can present energy $E_{\rm DW} = \int_{-\infty}^{+\infty}\mathcal{E}{\rm d}x$ of this domain wall in form

$$E_{\rm DW} = 8\int\limits_0^\pi \sin\theta\sqrt{1+\epsilon\cos^2 2\theta}\,{\rm d}\theta - 2\pi d. \tag{S19}$$

The condition $E_{\rm DW} < 0$, or equivalently

$$d > d_c^{\rm N}(\epsilon) = \frac{8}{\pi}\int\limits_0^1\sqrt{1+\epsilon(2\xi^2-1)^2}{\rm d}\xi, \tag{S20}$$

determines the area of parameters, where nucleation of the $2\pi$-domain wall on the background of the saturated state $\mathbf{n} = \hat{\boldsymbol{z}}$ is energetically preferable.

The general case $C > 0$ corresponds to the helical state, which can be interpreted as a periodical sequence of the considered domain walls. If $\epsilon = 0$ [2], then the solution of (S18) reads

$$\theta = 2\,{\rm am}\left(\sqrt{C}(x-x_0)\middle|-\frac{1}{C}\right), \tag{S21}$$

where ${\rm am}(x|k)$ is Jacobi's amplitude function [3] and the integration constant $x_0$ determines a uniform shift along $x$-axis. The solution (S21) determines period of the magnetization components $\mathrm{n}_x = \sin\theta$ and $\mathrm{n}_z = \cos\theta$:

$$T = \frac{2}{\sqrt{C}}{\rm K}\left(-\frac{1}{C}\right), \tag{S22}$$

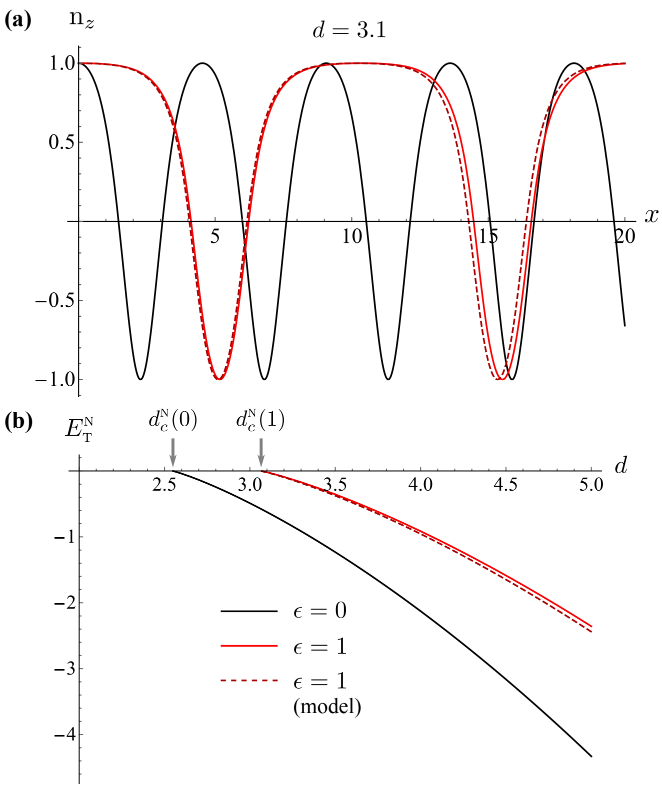


FIG. S1. Influence of the $\epsilon$-term on 1D periodical structure. (a) – perpendicular magnetization component $\mathrm{n}_z$; (b) – energy per period. The dashed line corresponds to the approximations: (a) the solution of Eq. (S18) with $C = \tilde{C}$, where $\tilde{C}$ is determined by (S24); (b) $\tilde{E}_{\mathrm{T}}^{\mathrm{N}} = -4\tilde{C}$.

where $\mathrm{K}(k)$ is complete elliptic integral of the first kind [3]. The constant $C$ must be found from the minimization of the total energy per period $E_{\mathrm{T}}^{\mathrm{N}} = T^{-1}\int_0^T \mathcal{E}\,\mathrm{d}x$. Performing the minimization procedure for (S21) and (S22) one obtains $E_{\mathrm{T}}^{\mathrm{N}} = -4C$ for energy of the equilibrium structure, where the equilibrium value of the constant $C$ is determined by the equation

$$\frac{d}{d_c^{\mathrm{N}}(0)} = \sqrt{C}\,\mathrm{E}\left(-\frac{1}{C}\right) \tag{S23}$$

with $\mathrm{E}(k)$ being the complete elliptic integral of the second kind. The total energy (8) per period reads $E_{\mathrm{1D}}^{\mathrm{N}} = ALE_{\mathrm{T}}^{\mathrm{N}}$. An example of a solution for the case $\epsilon = 0$ is shown in Fig. S1(a) by the black line.

For the case $\epsilon > 0$, the solution of Eq. (S18), which minimizes the energy $E_{\mathrm{T}}^{\mathrm{N}}(C)$ with respect to $C$ can be found only numerically. An example for the case $\epsilon = 1$ is shown in Fig. S1(a) by the red solid line. As one can see, the $\epsilon$-term can noticeably increase period of the structure. It is important to note that one can avoid the tedious procedure of the numerical minimization of the energy $E_{\mathrm{T}}^{\mathrm{N}}(C)$ by using the fact that the equilibrium value $C \approx \tilde{C}$, where $\tilde{C}$ is found in the way analogous to (S23):

$$\frac{d}{d_c(\epsilon)} = \sqrt{\tilde{C}}\,\mathrm{E}\left(-\frac{1}{\tilde{C}}\right). \tag{S24}$$

An example of such an approximate solution is shown in Fig. S1(a) by the red dashed line. And the corresponding energy per period can be well approximated as $E_{\mathrm{T}}^{\mathrm{N}} \approx -4\tilde{C}$, see Fig. S1(b).

Let us now proceed to the case $\mathscr{E}_{\mathrm{DMI}} = \mathscr{E}_{\mathrm{DMI}}^{\mathrm{B}}$. In this case the energy density coincides with (S14) but the DMI-term

$$\begin{aligned}\mathcal{E}_{\mathrm{1D}}^{\mathrm{B}} =&\theta'^2 + \sin^2\theta\phi'^2 + \epsilon\left(\cos\theta\cos\phi\theta' - \sin\theta\sin\phi\phi'\right)^2\\ &+ d\left(\sin\phi\theta' + \sin\theta\cos\theta\cos\phi\phi'\right) + 2(1-\cos\theta).\end{aligned} \tag{S25}$$

Energy expression (S25) generates the Euler-Lagrange equations

$$\begin{aligned}\theta'' - \sin\theta\cos\theta\phi'^2 - \epsilon\cos\theta\cos\phi\,\Xi& \qquad \text{(S26a)}\\ + d\sin^2\theta\cos\phi\phi' - \sin\theta = 0&,\\ \left(\sin^2\theta\phi'\right)' + \epsilon\sin\theta\sin\phi\Xi - d\sin^2\theta\cos\phi\theta' = 0&, \qquad \text{(S26b)}\end{aligned}$$

which coincide with (S15) up to the replacement $\sin\phi \leftrightarrow -\cos\phi$ in the DMI terms. As a result, equation (S26b) is satisfied when $\cos\phi = 0$ (in this case $\Xi = 0$), or in the other words $\mathrm{n}_x = 0$. Thus, the magnetization lies within the plane $\hat{\boldsymbol{y}}0\hat{\boldsymbol{z}}$. The latter corresponds to the Bloch domain walls. The components $\mathrm{n}_y = \sin\theta$ and $\mathrm{n}_z = \cos\theta$ are determined by the equation (S26a), which coincides with (S16) if $\epsilon = 0$. Thus, $\epsilon$ does not effect the static 1D solution for the case $\mathscr{E}_{\mathrm{DMI}} = \mathscr{E}_{\mathrm{DMI}}^{\mathrm{B}}$ and the further analysis coincides with the one done for $\mathscr{E}_{\mathrm{DMI}} = \mathscr{E}_{\mathrm{DMI}}^{\mathrm{N}}$ with $\epsilon = 0$.

### Skyrmion solutions

Let us consider two-dimensional solutions. As previously, we first consider the case $\mathscr{E}_{\mathrm{DMI}} = \mathscr{E}_{\mathrm{DMI}}^{\mathrm{N}}$. Introducing the normalized in-plane magnetization component $\boldsymbol{\eta} = \cos\phi\hat{\boldsymbol{x}} + \sin\phi\hat{\boldsymbol{y}}$ one can present the energy density in the form

$$\begin{aligned}\mathcal{E}_{\mathrm{2D}}^{\mathrm{N}} =&(\boldsymbol{\nabla}\theta)^2 + \sin^2\theta(\boldsymbol{\nabla}\phi)^2 + \epsilon\left[\boldsymbol{\nabla}\cdot(\sin\theta\boldsymbol{\eta})\right]^2\\ &+ 2d\,\sin^2\theta\,(\boldsymbol{\eta}\cdot\boldsymbol{\nabla}\theta) + 4\sin^2\frac{\theta}{2}.\end{aligned} \tag{S27}$$

The corresponding Euler-Lagrange equations $\delta E_{\mathrm{eff}}/\delta\theta = 0$ and $\delta E_{\mathrm{eff}}/\delta\phi = 0$ read

$$\begin{aligned}&\nabla^2\theta + \epsilon\cos^2\theta\,\boldsymbol{\nabla}\cdot\left[\boldsymbol{\eta}\left(\boldsymbol{\nabla}\theta\cdot\boldsymbol{\eta}\right)\right] \qquad \text{(S28a)}\\ &-\sin\theta\cos\theta\left\{(\boldsymbol{\nabla}\phi)^2 + \epsilon\left[(\boldsymbol{\nabla}\theta\cdot\boldsymbol{\eta})^2 - \boldsymbol{\eta}\cdot\boldsymbol{\nabla}(\boldsymbol{\nabla}\cdot\boldsymbol{\eta})\right]\right\}\\ &+ d\sin^2\theta\boldsymbol{\nabla}\cdot\boldsymbol{\eta} - \sin\theta = 0,\\ &\boldsymbol{\nabla}\cdot\left[\sin^2\theta\boldsymbol{\nabla}\phi\right] - d\sin^2\theta(\bar{\boldsymbol{\eta}}\cdot\boldsymbol{\nabla}\theta) \qquad \text{(S28b)}\\ &+ \epsilon\sin^2\theta\left[\bar{\boldsymbol{\eta}}\cdot\boldsymbol{\nabla}(\boldsymbol{\nabla}\cdot\boldsymbol{\eta}) - (\boldsymbol{\nabla}\theta\cdot\boldsymbol{\eta})(\boldsymbol{\nabla}\theta\cdot\bar{\boldsymbol{\eta}})\right]\\ &+ \epsilon\sin\theta\cos\theta\left[(\boldsymbol{\nabla}\theta\cdot\bar{\boldsymbol{\eta}})\boldsymbol{\nabla}\cdot\boldsymbol{\eta} + \bar{\boldsymbol{\eta}}\cdot\boldsymbol{\nabla}(\boldsymbol{\nabla}\theta\cdot\boldsymbol{\eta})\right] = 0,\end{aligned}$$

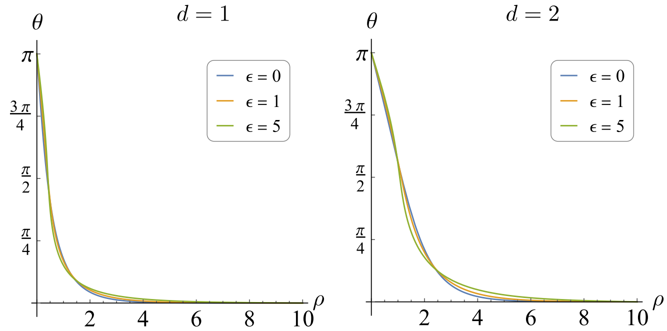


FIG. S2. Skyrmion profiles determined by Eq. (9) for various values of parameters $d$ and $\epsilon$.

where $\bar{\boldsymbol{\eta}} = \partial_\phi \boldsymbol{\eta} = -\sin\phi\hat{\boldsymbol{x}} + \cos\phi\hat{\boldsymbol{y}}$ is the unit vector perpendicular to $\boldsymbol{\eta}$. Equations (S28) have trivial solution $\theta = 0$. Besides, the Eq. (S28b) is always satisfied if $\boldsymbol{\eta} = \mathbf{const}$ and $\theta = \theta(\xi)$ with $\xi$ being a coordinate along $\boldsymbol{\eta}$. This is the one-dimensional case considered in the previous section. The analogous "one-dimensional" solution takes place in the curvilinear polar frame of reference $\{\rho, \chi\}$. Indeed, in this case the Eq. (S28b) is satisfied if $\boldsymbol{\eta} = \boldsymbol{e}_\rho$ (equivalently $\phi = \chi$) and $\theta = \theta(\rho)$. Herewith, Eq. (S28a) is reduced to Eq. (9), which describes profile of the isolated skyrmion. Note that for the case $d < 0$ the in-plane magnetization is $\boldsymbol{\eta} = -\boldsymbol{e}_\rho$ (equivalently $\phi = \chi + \pi$). Few examples of skyrmion profiles determined by Eq. (9) for various values of parameters $d$ and $\epsilon$ are shown in Fig. S2. Note that the skyrmion size is mainly determined by the parameter $d$, while the parameter $\epsilon$ weakly modifies details of the skyrmion profile.

Let us now consider stability of the static skyrmion solutions of Eq. (9). To this end we introduce small deviations $\theta = \theta_0 + \vartheta$ and $\phi = \phi_0 + \varphi/\sin\theta_0$ of the static profile $\theta_0 = \theta_0(\rho)$, $\phi_0 = \chi$. Landau-Lifshitz equations $\sin\theta\partial_t\phi = \frac{\gamma}{M_s}\delta E_{\text{eff}}/\delta\theta$, $-\sin\theta\partial_t\theta = \frac{\gamma}{M_s}\delta E_{\text{eff}}/\delta\phi$ linearized in vicinity of the static solution with respect to the deviations $\vartheta$ and $\varphi$ are as follows

$$\begin{aligned} \dot{\varphi} &= \hat{\mathrm{H}}_1\vartheta + W_1\partial_\chi\varphi + V\partial^2_{\rho\chi}\varphi, \\ -\dot{\vartheta} &= \hat{\mathrm{H}}_2\varphi - W_2\partial_\chi\vartheta + V\partial^2_{\rho\chi}\vartheta, \end{aligned} \tag{S29}$$

where dot indicates the derivative with respect to the dimensionless time $\tau = t\Omega_0$ with $\Omega_0 = \gamma H$ being the Larmor frequency. The differential operators and the potentials read

$$\begin{aligned} \hat{\mathrm{H}}_1 &= -\nabla^2_\rho - \frac{\epsilon}{\rho}\partial_\rho\left(\rho\cos^2\theta_0\partial_\rho\right) - \frac{1}{\rho^2}\partial^2_{\chi\chi} + U_1, \\ \hat{\mathrm{H}}_2 &= -\nabla^2_\rho - \frac{1+\epsilon}{\rho^2}\partial^2_{\chi\chi} + U_2, \\ U_1 &= \cos 2\theta_0\left(\frac{1+\epsilon}{\rho^2} + \epsilon\,\theta_0'^2\right) + \epsilon\sin 2\theta_0\nabla^2_\rho\theta_0 \\ &- \frac{d}{\rho}\sin 2\theta_0 + \cos\theta_0, \\ U_2 &= (1+\epsilon)(\cot\theta_0\nabla^2_\rho\theta_0 - \theta_0'^2) - \frac{\epsilon}{\rho^2} - d\theta_0', \\ W_1 &= \frac{2+\epsilon}{\rho^2}\cos\theta_0 - \frac{d}{\rho}\sin\theta_0, \\ W_2 &= W_1 - \frac{\epsilon}{\rho}\sin\theta_0\theta_0', \qquad V = -\frac{\epsilon}{\rho}\cos\theta_0. \end{aligned} \tag{S30}$$

Note that term $(\boldsymbol{\nabla}\cdot\mathbf{n})^2$ leads to the mixing of the derivatives in the linearized equations (S29) (the $V$-term). This is in contrast to the corresponding linear equations previously obtained for magnons over precessional solitons in easy-axis magnets [4–6], magnetic vortices in easy-plane magnets [7, 8], and magnetic skyrmions [9, 10].

Equations (S29) have solution $\vartheta = f(\rho)\cos(\omega\tau + \mu\chi + \chi_0)$, $\varphi = g(\rho)\sin(\omega\tau + \mu\chi + \chi_0)$, where $\mu \in \mathbb{Z}$ is azimuthal quantum number and $\chi_0$ ia an arbitrary phase. The eigenfrequencies $\omega$ and the corresponding eigenfunctions $f$, $g$ are determined by the following generalized eigen-value problem (EVP)

$$\hat{\mathcal{H}}\boldsymbol{\psi} = \omega\hat{\sigma}_x\boldsymbol{\psi}, \quad \hat{\mathcal{H}} = \begin{Vmatrix} \hat{\mathscr{H}}_1 & \mu(W_1 + V\partial_\rho) \\ \mu(W_2 - V\partial_\rho) & \hat{\mathscr{H}}_2 \end{Vmatrix} \tag{S31}$$

where $\boldsymbol{\psi} = (f, g)^{\mathrm{T}}$ and $\hat{\sigma}_x$ is the first Pauli matrix. The diagonal operators are as follows

$$\begin{aligned} \hat{\mathscr{H}}_1 &= -\nabla^2_\rho - \frac{\epsilon}{\rho}\partial_\rho\left(\rho\cos^2\theta_0\partial_\rho\right) + \frac{\mu^2}{\rho^2} + U_1 \\ \hat{\mathscr{H}}_2 &= -\nabla^2_\rho + \frac{(1+\epsilon)\mu^2}{\rho^2} + U_2. \end{aligned} \tag{S32}$$

EVP (S31) was solved numerically for a range of $d$ and a couple of values of $\epsilon$, see Fig. 1(a) and discussion in the main text.

For the case $\mathscr{E}_{\text{DMI}} = \mathscr{E}^{\text{B}}_{\text{DMI}}$ the energy expression coincides with (S27), but the DMI term

$$\begin{aligned} \mathcal{E}^{\text{B}}_{\text{2D}} =& (\boldsymbol{\nabla}\theta)^2 + \sin^2\theta(\boldsymbol{\nabla}\phi)^2 + \epsilon\left[\boldsymbol{\nabla}\cdot(\sin\theta\boldsymbol{\eta})\right]^2 \\ &+ 2d\,\sin^2\theta\left[\boldsymbol{\nabla}\theta\times\boldsymbol{\eta}\right]_z + 4\sin^2\frac{\theta}{2}. \end{aligned} \tag{S33}$$

The corresponding Euler-Lagrange equations coincide with (S28), where the replacement $\boldsymbol{\eta} \leftrightarrow \bar{\boldsymbol{\eta}}$ is made in the DMI term (and only in this term). The second equation is satisfied if $\boldsymbol{\eta} = \boldsymbol{e}_\chi$, this corresponds to a Bloch skyrmion. The skyrmion profile is determined by the first equation, which in this case coincides with Eq. (9) with $\epsilon = 0$. Thus, $\epsilon$ has no influence on static profiles of the Bloch skyrmion.

The corresponding linearized Landau-Lifshitz equations coincide with (S29) but the form of the differential operators and potentials

$$\begin{aligned}
\hat{\mathrm{H}}_1 &= -\nabla_\rho^2 - \frac{1+\epsilon\cos^2\theta_0}{\rho^2}\partial_{\chi\chi}^2 + U_1,\\
\hat{\mathrm{H}}_2 &= -(1+\epsilon)\nabla_\rho^2 - \frac{1}{\rho^2}\partial_{\chi\chi}^2 + U_2,\\
U_1 &= \frac{\cos 2\theta_0}{\rho^2} - d\frac{\sin 2\theta_0}{\rho} + \cos\theta_0,\\
U_2 &= \cot\theta_0\nabla_\rho^2\theta_0 - \theta_0'^2 + \frac{\epsilon}{\rho^2} - d\theta_0',\\
W_1 &= \frac{2+\epsilon}{\rho^2}\cos\theta_0 - \frac{d}{\rho}\sin\theta_0,\\
W_2 &= W_1 + \frac{\epsilon}{\rho}\sin\theta_0\theta_0', \qquad V = \frac{\epsilon}{\rho}\cos\theta_0.
\end{aligned} \tag{S34}$$

As for the previous case, the solution of the linear problem is reduced to a generalized EVP, which coincides with (S31) but the potentials are determined by (S34) and the diagonal operators are as follows

$$\begin{aligned}
\hat{\mathscr{H}}_1 &= -\nabla_\rho^2 + \frac{\mu^2(1+\epsilon\cos^2\theta_0)}{\rho^2} + U_1\\
\hat{\mathscr{H}}_2 &= -(1+\epsilon)\nabla_\rho^2 + \frac{\mu^2}{\rho^2} + U_2.
\end{aligned} \tag{S35}$$

The corresponding EVP (S31) was solved numerically for a range of $d$ and a couple of values of $\epsilon$, see Fig. 1(b) and discussion in the main text.


[1] Stefan Rex, Flavio S. Nogueira, and Asle Sudbø, "Topological magnetic dipolar interaction and nonlocal electric magnetization control in topological insulator heterostructures," Physical Review B **94**, 020404(R) (2016).

[2] The case $\epsilon = 0$ was analysed earlier in Ref. [11].

[3] Milton Abramowitz and Irene A. Stegun, *Handbook of mathematical functions with formulas, graphs, and mathematical tables*, ninth Dover printing, tenth GPO printing ed. (Dover, New York, 1972).

[4] D. D. Sheka, B. A. Ivanov, and F. G. Mertens, "Internal modes and magnon scattering on topological solitons in two–dimensional easy–axis ferromagnets," Phys. Rev. B **64**, 024432 (2001).

[5] B. A. Ivanov and D. D. Sheka, "Local magnon modes and the dynamics of a small–radius two–dimensional magnetic soliton in an easy-axis ferromagnet," JETP Lett. **82**, 436–440 (2005).

[6] D. D. Sheka, C. Schuster, B. A. Ivanov, and F. G. Mertens, "Dynamics of topological solitons in two-dimensional ferromagnets," The European Physical Journal B - Condensed Matter **50**, 393–402 (2006).

[7] B. A. Ivanov, H. J. Schnitzer, F. G. Mertens, and G. M. Wysin, "Magnon modes and magnon-vortex scattering in two-dimensional easy-plane ferromagnets," Phys. Rev. B **58**, 8464–8474 (1998).

[8] Denis D. Sheka, Ivan A. Yastremsky, Boris A. Ivanov, Gary M. Wysin, and Franz G. Mertens, "Amplitudes for magnon scattering by vortices in two–dimensional weakly easy–plane ferromagnets," Phys. Rev. B **69**, 054429 (2004).

[9] Christoph Schütte and Markus Garst, "Magnon-skyrmion scattering in chiral magnets," Phys. Rev. B **90**, 094423 (2014).

[10] Volodymyr P. Kravchuk, Denis D. Sheka, Ulrich K. Rößler, Jeroen van den Brink, and Yuri Gaididei, "Spin eigenmodes of magnetic skyrmions and the problem of the effective skyrmion mass," Phys. Rev. B **97**, 064403 (2018).

[11] A. Bogdanov and A. Hubert, "Thermodynamically stable magnetic vortex states in magnetic crystals," Journal of Magnetism and Magnetic Materials **138**, 255–269 (1994).